Published OnlineFirst April 17, 2019; DOI: 10.1158/0008-5472.CAN-18-2540

Translational Science

Cancer Research

Activation of the Unfolded Protein Response via Inhibition of Protein Disulfide Isomerase Decreases the Capacity for DNA Repair to Sensitize Glioblastoma to Radiotherapy

Yajing Liu[1], Wenbin Ji[1], Andrea Shergalis[2], Jiaqi Xu[1,3], Amy M. Delaney[1], Andrew Calcaterra[1], Anupama Pal[1], Mats Ljungman[1,4], Nouri Neamati[2], and Alnawaz Rehemtulla[1]

Abstract

Patients with glioblastoma multiforme (GBM) survive on average 12 to 14 months after diagnosis despite surgical resection followed by radiotheraphy and temozolomide therapy. Intrinsic or acquired resistance to chemo- and radiotherapy is common and contributes to a high rate of recurrence. To investigate the therapeutic potential of protein disulfide isomerase (PDI) as a target to overcome resistance to chemoradiation, we developed a GBM tumor model wherein conditional genetic ablation of prolyl 4-hydroxylase subunit beta (P4HB), the gene that encodes PDI, can be accomplished. Loss of PDI expression induced the unfolded protein response (UPR) and decreased cell survival in two independent GBM models. Nascent RNA Bru-seq analysis of PDI-depleted cells revealed a decrease in transcription of genes involved in DNA repair and cell-cycle regulation. Activation of the UPR also led to a robust decrease in RAD51 protein expression as a result of its ubiquitination-mediated proteosomal degradation. Clonogenic survival assays demonstrated enhanced killing of GBM cells in response to a combination of PDI knockdown and ionizing radiation (IR) compared with either modality alone, which correlated with a decreased capacity to repair IR-induced DNA damage. Synergistic tumor control was also observed with the combination of PDI inhibition and IR in a mouse xenograft model compared with either single agent alone. These findings provide a strong rationale for the development of PDI inhibitors and their use in combination with DNA damage-inducing, standard-of-care therapies such as IR.

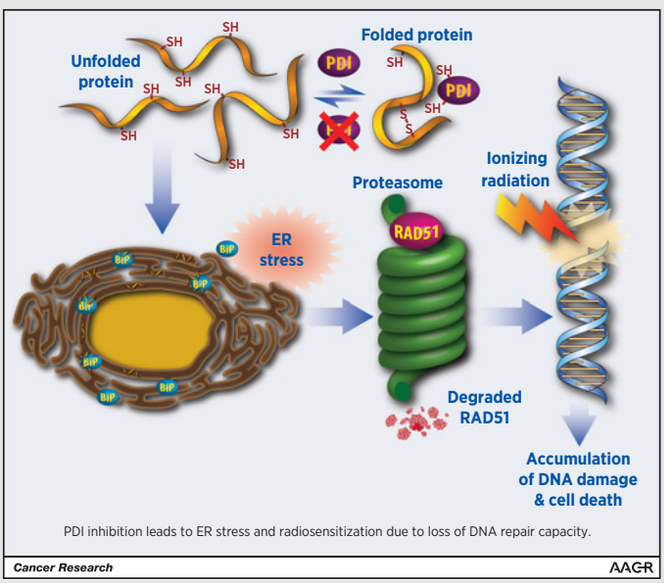

Significance: These findings identify PDIA1 as a therapeutic target in GBM by demonstrating efficacy of its inhibition in combination with radiotherapy through a novel mechanism involving downregulation of DNA repair genes.

Graphical Abstract: http://cancerres.aacrjournals.org/content/canres/79/11/2923/F1.large.jpg.

[1]Department of Radiation Oncology, University of Michigan Medical School and Rogel Cancer Center, Ann Arbor, Michigan. [2]Department of Medicinal Chemistry, College of Pharmacy, and Rogel Cancer Center, University of Michigan, Ann Arbor, Michigan. [3]Weill Cornell Graduate School of Medical Sciences, New York, New York. [4]Department of Environmental Health Sciences, School of Public Health, University of Michigan, Ann Arbor, Michigan.

Note: Supplementary data for this article are available at Cancer Research Online (http://cancerres.aacrjournals.org/).

Corresponding Author: Alnawaz Rehemtulla, University of Michigan Medical School, 1600 Huron Parkway, Ann Arbor, MI 48109. Phone: 734-764-4209; E-mail: alnawaz@med.umich.edu

Cancer Res 2019;79:2923–32

doi: 10.1158/0008-5472.CAN-18-2540

Published OnlineFirst April 17, 2019; DOI: 10.1158/0008-5472.CAN-18-2540

Introduction

Glioblastoma multiforme (GBM) is the most common and lethal primary malignant brain tumor (1). The standard of care treatment for GBM involves maximal tumor resection followed by adjuvant temozolomide combined with radiotherapy. This combination demonstrates a modest improvement in median survival to 15 months compared with 12 months with radiation alone (2, 3). Tumor recurrence occurs in most patients with GBM, resulting in an average 5-year survival rate of only 5% (4). Genetic profiling has identified recurrent copy number alterations and/or mutations in EGFR, neurofibromin 1 (NF1), platelet-derived growth factor receptor alpha (PDGFRA)/isocitrate dehydrogenase [NADP(+)] 1 (IDH1), TP53, PI3K complex, and cyclin-dependent kinase inhibitor 2A (CDKN2A; refs. 3, 5–7). Although the mechanistic basis for the contribution of these mutations to oncogenesis is becoming better understood, therapeutic approaches to target several of these pathways have limited benefit in clinical trials (3, 8–13). The fact that GBM tumors show intratumoral heterogeneity may at least partially contribute to the dismal outcomes of therapeutic targeting of commonly dysregulated oncogenic pathways. Therefore, there is an urgent need to develop therapies that target pathways required for survival of glioblastoma, irrespective of oncogenic mutation status.

Because of the high rate of protein synthesis in cancer cells, an enhanced capacity for protein folding is required, which puts major demand on the protein folding machinery in the endoplasmic reticulum (ER). To accommodate such demand, upregulation of proteins such as PDI is often observed (3). The PDI family consists of 21 enzymes that catalyze disulfide bond formation, reduction, and isomerization to ensure proper folding of nascent polypeptides (14), and also act as chaperones to assist protein folding (15). Several, but not all, of the PDI family members are primarily localized to the ER, the central compartment for protein folding and degradation, to maintain physiological homeostasis (16). In response to ER stress, an imbalance between the unfolded protein load and the protein folding machinery in the ER initiates a collection of signaling cascades termed the unfolded protein response (UPR) to restore a productive ER protein-folding environment by enhancing the capacity for protein folding and transport (17, 18). Expression of PDIA1, the canonical member of the PDI family, is upregulated in brain and central nervous system cancers compared with matched normal tissues (19). In addition, proteomic analysis has revealed upregulation of the PDI in many cancers (20–22). Furthermore, serial *in vivo* transplantation of primary glioma reveals PDI overexpression in invasive low-generation tumors (23). We hypothesized that the dependence of tumor cells on PDI activity provides a rationale for its therapeutic targeting in GBM, irrespective of oncogenic mutation status. We recently described propynoic acid carbamoyl methyl amides (PACMA) as irreversible inhibitors of PDI, a first-in-class, safe, and efficacious targeted anticancer agents (24), as well as second-generation PDI inhibitors BAP2 (25). Because the prolyl 4-hydroxylase subunit beta (*P4HB*) gene family that encodes PDI proteins, comprises 21 genes, varying in size, expression, localization, and enzymatic function (26), of which PDIA1 is believed to be the most highly expressed in GBM (19) and the primary target of our current small molecule agents, it is essential that we demonstrate the selective dependence of GBM cells on PDI to validate it as a therapeutic target.

Materials and Methods

Cell lines and treatment

U87 (purchased from ATCC) and D54 (27, 28) cells were maintained in DMEM (VWR; Corning) and RPMI (Life Technologies; Gibco) respectively, supplemented with 10% (v/v) FBS (GE Healthcare; Hyclone). The cells were authenticated using short tandem repeat profiling (tested on 12/3/18), and routinely tested for *Mycoplasma* contamination (latest test on November 26, 2018) with MycoAlert Mycoplasma Detection Kit (Lonza). All cells used in the experiments were thawn within 10 passages and were maintained *in vitro* no more than 2 months.

For tunicamycin and MG132 (both from Sigma-Aldrich) treatment, cells were seeded overnight, and tunicamycin (5 μg/mL) was added with or without MG132 (10 μmol/L) for 16 hours. For DNA repair studies, D54 and U87 cells were plated at 100,000 cells/well onto 0.1% poly-L-lysine (Sigma) coated four-well Millicell EZ slides (Millipore Sigma) overnight followed by 3 days of PDIA1 shRNA induction. Subsequently, 2 Gy IR was delivered using an IC-320 orthovoltage irradiator (Kimtron Medical) and the cells were fixed at 0.5, 4, 8, 16, and 24 hours post-irradiation. Cycloheximide (Calbiochem) was used at 100 μg/mL for 0, 2, 4, 6, and 8 hours for the time-course assay to study protein degradation.

LentiCRISPR sgP4HB cloning and production

Two single-guide RNAs (sgRNA) for P4HB: 5′-CACCGCCGCGCACGCCGTACTGCT-3′ and 5′-CACCGAAGCAACTTCGCGGAGGCGC-3′ identified computationally (https://zlab.bio/guide-design-resources) were inserted into the lentiCRISPR v2 plasmid (Addgene). Briefly, vector and annealed oligos were digested by BsmBI (NEB) and ligated using the Quick Ligation Kit (NEB), and transformed into Stbl3 bacteria (Invitrogen). Single colonies were expanded and sequenced to confirm sgRNA insertion, and identified recombinant clones were packaged in HEK293T cells with psPAX2 and pCMV-VSV-G as previously described (Addgene; refs. 29, 30).

Lentivirus infection

The inducible pTripz-PDIA1 shRNA vectors were obtained from Dharmacon Open Biosystems. Lentivirus was produced using HEK293T cells at the University of Michigan Vector Core Facility. U87 and D54 cells were infected in the presence of polybrene (8 μg/mL; AmericanBio), and stable cells were selected by single colony isolation in the presence of puromycin (1 μg/mL; InvivoGen).

Bru-Seq

Nascent RNA Bru-seq was performed as previously described (31). Gene set enrichment analyses (GSEA) based on a transcriptional cut-off of >0.1 reads per kilobase of transcript, per million mapped reads (RPKM) and >100 counts per gene.

Clonogenic assay

Doxycycline (2 μg/mL; Sigma-Aldrich) was added to stable D54 and U87 cells to induce PDIA1 shRNA for 3 days. Cells were irradiated with 0, 2, 4, 6, or 8 Gy as a single dose and plated the

Published OnlineFirst April 17, 2019; DOI: 10.1158/0008-5472.CAN-18-2540

following day at a clonogenic density with fresh medium (without doxycycline) for 7 to 14 days before the colonies were fixed with 4% paraformaldehyde (Electron Microscopy Science) and stained using 0.1% Crystal Violet (Sigma-Aldrich).

qPCR

PDI shRNA was induced for 1 to 3 days in D54 and U87 stable cells and total RNA was extracted using the Qiagen RNeasy Kit (Qiagen). One microgram of total RNA was reverse-transcribed into cDNA using the High-Capacity cDNA Reverse Transcription Kit (Applied Biosystems). qPCR was performed using SYBR Green Master Mix (Bio-Rad) on a Mastercycler RealPlex^2 (Eppendorf) with denaturation at 95°C for 15 minutes followed by 40 cycles of amplification at 94°C for 15 seconds; 55°C for 30 seconds; 72°C for 30 seconds. Sequences of the primers are listed in Supplementary Table S1. Relative expression levels were normalized to GAPDH and fold changes in mRNA expression level were evaluated using the $\Delta\Delta C_t$ method.

Western blot analysis

Cells or snap-frozen tissues were lysed in RIPA buffer consisting of 150 mmol/L NaCl, 1 mmol/L EDTA (pH 8.0), 50 mmol/L Tris-HCl (pH 8.0), 1% NP-40 (v/v), 0.25% sodium deoxycholate (w/v), 0.1% SDS (w/v; all from Sigma-Aldrich), supplemented with PhosSTOP Phosphatase Inhibitor Cocktail and cOmplete Protease Inhibitor Cocktail (Roche), and sonicated with a Sonic Dismembrator Model 100 (Thermo Fisher Scientific). Western blotting was performed as described previously (32), using primary antibodies to PDI, BIP, elF2α, p-elF2α (S51), RAD51, phospho-Histone H2AX (Ser139;

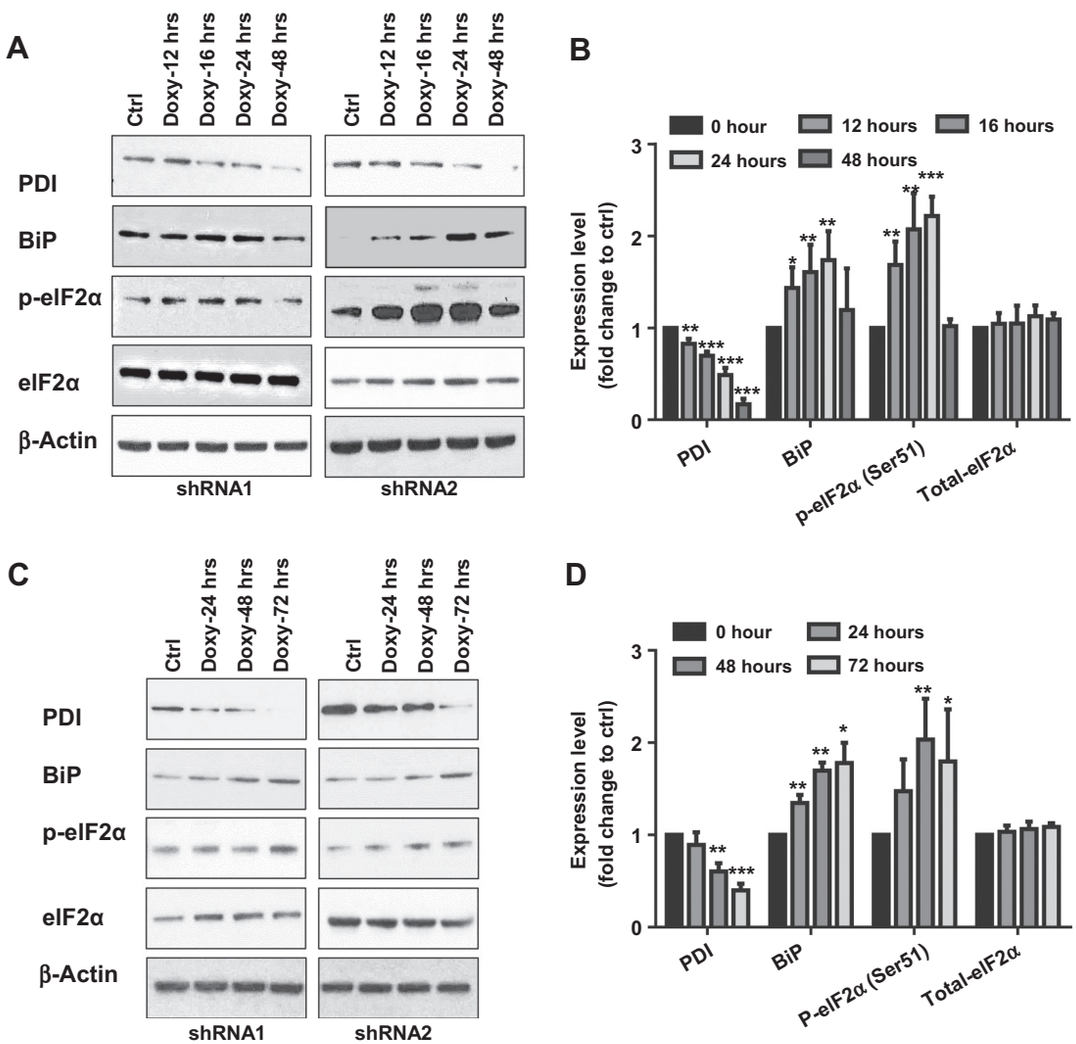

Figure 1.

PDI inhibition induces ER stress in GBM cells. PDIA1 KD was induced in D54 by adding doxycycline (2 μg/mL; **A**), and the lysates were collected after 12, 16, 24, and 48 hours and ER stress markers were quantified (**B**). Doxycycline (2 μg/mL) was added to U87 cells (**C**) for 24, 48, and 72 hours to induce PDIA1 shRNA and the lysates were collected for ER stress marker quantification (**D**). Protein expression level was normalized against β-actin. Data are means ± SD from three independent experiments. *, $P < 0.05$; **, $P < 0.01$; ***, $P < 0.001$.

Published OnlineFirst April 17, 2019; DOI: 10.1158/0008-5472.CAN-18-2540

all from Cell Signaling Technology), and β-actin (Sigma). Horseradish peroxidase-conjugated goat anti-rabbit IgG (H+L) and goat anti-mouse (H+L; Jackson ImmunoResearch) were applied as secondary antibodies and Pierce ECL (Thermal Scientific) or ECL prime (GE Healthcare) were used as substrate (detailed antibody working concentrations are listed in Supplementary Table S2).

Immunofluorescent staining

Cells were fixed in 4% paraformaldehyde (Electron Microscopy Science) for 15 minutes at room temperature and washed with 1× PBS before permeabilization in 0.3% Triton X-100 (Sigma-Aldrich) for 10 minutes at room temperature. The slides were blocked in 10% goat serum (Reagent A from Invitrogen Histostain-Plus Kit) for 30 minutes and γH2AX-AF488 (Millipore) was applied at 1:100 dilution in 1% blocking solution overnight. ProLong Gold with DAPI (Invitrogen) were used to prepare the slides for analysis using an Olympus BX-51 scope. γ-H2AX signal was quantified using ImageJ software. More than 100 cells were analyzed per experiment per condition.

Xenograft mouse model of glioblastoma

A total of 1×10^6 U87-pTripz-PDIA1 shRNA stable cells in 100 μL DMEM (VWR; Corning): Matrigel (BD Bioscience; 1:1) suspension were subcutaneously injected into 6 to 8 weeks old NCRNU sp/sp mice (Taconic). Tumor size was monitored twice weekly and tumor volume was defined as $(L \times W \times W)/2$, where W is tumor width and L is tumor length. Mice were randomized into four groups when tumors reached around 100 mm^3 (five to eight animals/group), and two groups were switched to doxycycline (2 mg/mL) in 5% sucrose (both from Sigma-Aldrich) water (renewed thrice per week). Radiation was given at 2 Gy per day, 5 days a week for 2 weeks only to tumors using a IC-320 orthovoltage irradiator (Kimtron Medical). The rest of the body was protected by lead shielding. All animal experiments were approved by the University of Michigan Committee on the Use and Care of Animals.

Statistical analysis

ImageJ was used for protein quantification and all proteins were normalized against loading control. The statistical significance between two groups was evaluated based on two-tailed Student t test using GraphPad Prism (Version 7). P values <0.05 were considered statistically significant.

Results

PDI knockdown leads to ER stress in GBM cells

To elucidate the cellular response to PDI knockdown (KD), we generated stable GBM cell lines using D54 and U87 wherein doxycycline-inducible PDI shRNA expression can be achieved. Two shRNAs targeting distinct sequences were used for PDI KD. In D54 cells, downregulation of PDI with shRNA2 was evident as early as 12 hours after doxycycline treatment (1.2-fold decrease compared with control, $P = 0.0013$), with a 5.9-fold decrease at 48 hours post-induction (Fig. 1A and B). In U87 cells, the decrease in PDI protein levels started at 24 hours (1.1-fold decrease compared with control) but only became significant after 48 hours (1.7-fold deduction compared with control, $P = 0.0047$; Fig. 1C and D). We next explored whether downregulation of PDI leads to ER stress. Increased levels of BiP, a well characterized maker for ER stress (33), was observed as early as 12 hours after doxycycline treatment (1.4-fold increase compared with control, $P = 0.0105$) in D54 cells (Fig. 1A and C) and remained elevated at 24 hours (1.7-fold increase, $P = 0.0048$) post-shRNA2 induction. However, BiP returned to basal levels around 48 hours post-doxycycline treatment, despite a further decline in PDI protein expression. In U87 cells (Fig. 1C and D), upregulation of BiP was detected 24 hours after doxycycline addition (1.3-fold increase, $P = 0.0023$), and expression was maintained up to 72 hours (1.8-fold increase, $P = 0.0240$).

Upon ER stress, EIF2α is phosphorylated (p-EIF2α) at serine 51, leading to inhibition of protein translation and preventing further entry of nascent polypeptides into the ER (34). p-EIF2α levels were elevated 12 hours after initiation of *PDI* KD in D54

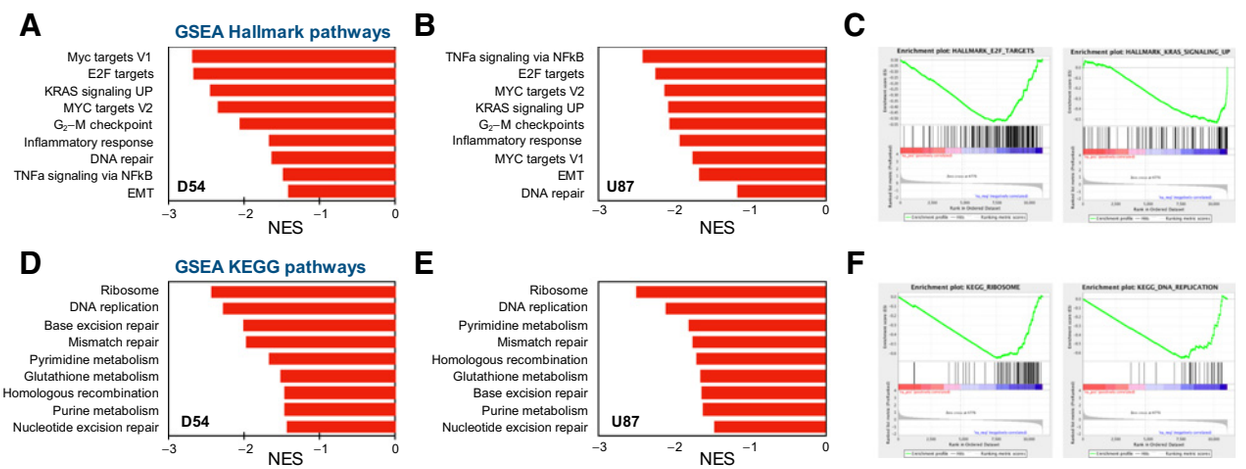

Figure 2.

GSEA analysis of PDI KD reveals reduced transcription of DNA repair genes, E2F1, MYC and targets, and KRAS signaling. Nascent RNA Bru-seq was used to assess the effect of 72-hour doxycycline-induced PDI KD on genome-wide transcription in D54 and U87 cells. GSEA of Hallmark pathways using $\log_2$-fold rank ordered genes from 10,687 and 11,030 genes expressed in D54 (**A**) and U87 (**B**) cells, respectively. **C,** GSEA plots for the top downregulated pathways: E2F1 targets and KRAS signaling. GSEA of KEGG pathways for D54 (**D**) and U87 (**E**) cells and GSEA plots for the top downregulated pathways: ribosome and DNA replication (**F**).

Published OnlineFirst April 17, 2019; DOI: 10.1158/0008-5472.CAN-18-2540

cells (1.7-fold increase compared with control, $P = 0.0026$) and remained elevated at 24 hours (2.2-fold increase, $P = 7 \times 10^{-4}$) but returned to basal levels after 48 hours (Fig. 1A and B). In U87 cells, p-EIF2α levels were significantly upregulated at 48 hours (2.0-fold increase, $P = 0.0090$) and remained elevated at 72 hours (1.8-fold increase, $P = 0.0380$; Fig. 1C and D), a pattern that correlated to changes observed for BiP and the dynamics of PDI downregulation in both cell lines.

PDI KD leads to decreased transcription of DNA repair genes

In response to unfolded proteins, dissociation of BiP from the ER membrane-spanning UPR receptor proteins, PERK, IRE1, and ATF6, results in transcriptional, translational, and posttranslational changes in gene expression to restore cellular homeostasis (35). To investigate immediate changes in gene transcription in response to *PDI* KD and resulting accumulation of unfolded proteins, we conducted genome-wide nascent RNA Bru-seq analysis (31). We found that KD of PDI expression for 72 hours resulted in transcriptional upregulation of 153 and 58 genes by greater than two-fold, whereas 135 and 41 genes were downregulated greater than two-fold in D54 and U87 cells, respectively. GSEA revealed that among the Hallmark pathways, MYC and E2F1 targets were suppressed as was KRAS signaling, G_2–M checkpoint, inflammatory response, and DNA repair in both cell lines (Fig. 2A–C). Furthermore, GSEA analysis of Kyoto Encyclopedia of Genes and Genomes (KEGG) pathways showed a marked suppression of ribosome and DNA replication as well as of four major DNA repair pathways and purine/pyrimidine and glutathione metabolism (Fig. 2D–F). RAD51, which plays a central role in homologous recombination repair (HR), showed a modest but significant reduction in transcription (Supplementary Fig. S1). To further investigate the effect of *PDI* KD on *RAD51* gene expression, total RNA was extracted 24, 48, and 72 hours after doxycycline treatment and analyzed for steady-state *PDIA1* and *RAD51* mRNA levels by qRT-PCR. Maximum KD of *PDIA1* mRNA was achieved in D54 and U87 cells after 72 hours of shRNA2 induction with a 5.6- and 4-fold downregulation of *PDIA1* mRNA ($P < 0.0001$), respectively. Downregulation of *RAD51* steady-state RNA expression was detected at 48 hours after PDI KD and reached approximately a 2.0-fold decrease compared with control at 72 hours ($P < 0.0001$). In addition, *GRP78*, the gene encoding BiP, showed significantly upregulated RNA expression ($P < 0.01$ and $P < 0.001$ in D54 and U87 cells, respectively; Fig. 3A and B), indicating induction of ER stress in response to PDI KD. Although Bru-seq and qRT-PCR analysis revealed a modest reduction of transcription and steady-state RNA levels, Western blot analysis revealed a robust downregulation of RAD51 protein levels (10-fold) after 48 hours and 72 hours in both D54 and U87 cells (Fig. 3C). To independently confirm the observation that *PDI* KD leads to ER stress and downregulation of

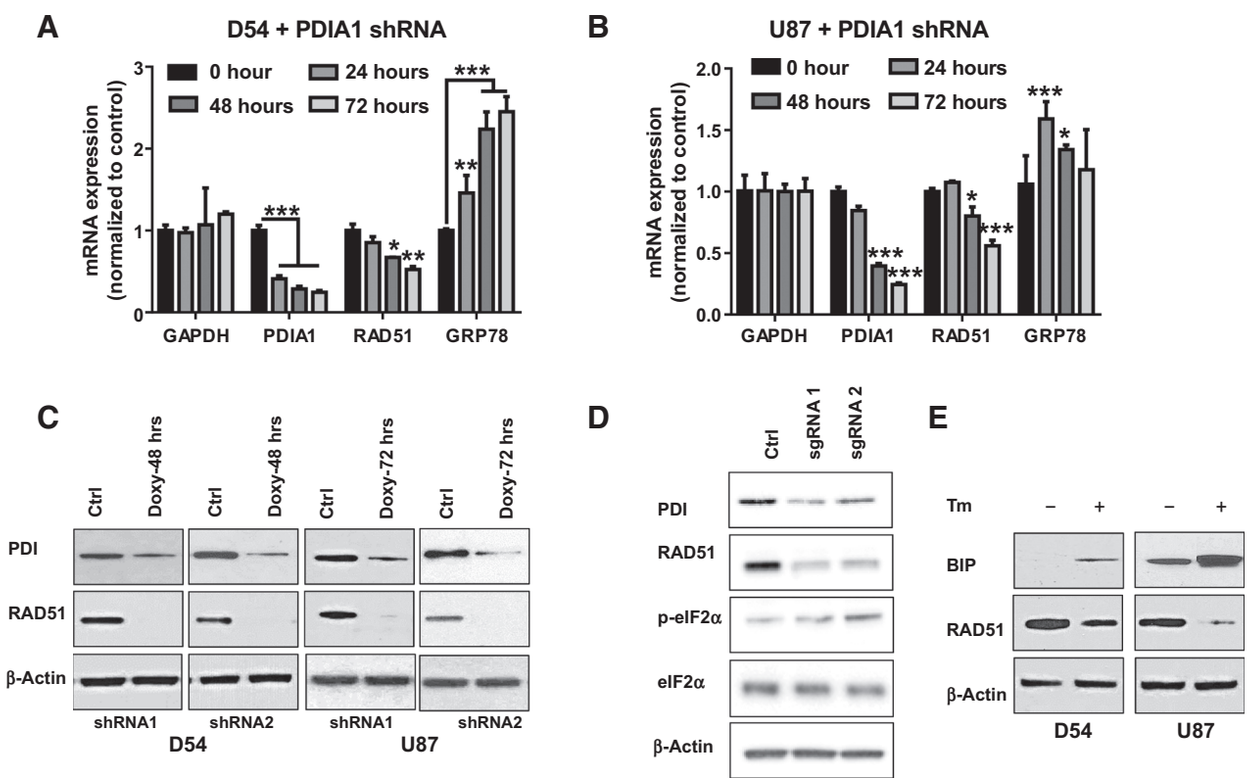

Figure 3.

PDI KD induces ER stress that downregulates RAD51. qPCR (**A** and **B**) and Western blot (**C**) analysis for PDI and RAD51 expression level after doxycycline induction as indicated. qPCR data are presented as means ± SD. *, $P < 0.05$; **, $P < 0.01$; ***, $P < 0.001$ from three independent experiments. **D,** Immunoblot analysis of CRISPR/Cas9 targeting *P4HB* U87 cells after 48 hours of infection. **E,** Tunicamycin (Tm) was added at 5 μg/μL to D54 and U87 cells for 12 hours and RAD51 and BiP protein expression were assessed.

Published OnlineFirst April 17, 2019; DOI: 10.1158/0008-5472.CAN-18-2540

RAD51, we performed CRISPR/Cas9, where sgRNA targeting *P4HB* exon was inserted into a lentiCRISPR vector (36). Analysis of cells after a short-term enrichment of infected cells using puromycin revealed that CRISPR/Cas9-mediated deletion of the *PDI* locus led to a simultaneous increase in ER stress as detected by an upregulation of phosphorylated eIF2α and a concomitant decrease in RAD51 levels (Fig. 3D). To investigate whether the downregulation of RAD51 occurred specifically as a consequence of *PDI* KD or as a general response of the UPR, GBM cells were treated with tunicamycin, a potent inhibitor of N-linked glycosylation and inducer of the UPR. Tunicamycin treatment resulted in BiP upregulation and a concomitant decrease in RAD51 protein levels after 12 hours (Fig. 3E). Thus, mRNA levels of RAD51, a key mediator of homologous recombination mediated DNA repair, were reduced in response to accumulation of unfolded proteins induced by either PDI KD or tunicamycin.

RAD51 is targeted by ubiquitin-mediated proteasomal degradation following ER stress

Upon ER stress, the UPR triggers three major cellular responses: inhibition of transcription and protein translation, upregulation of protein-folding capacity to maintain ER homeostasis and ER-associated protein degradation to eliminate misfolded proteins (ERAD; ref. 18). Because the robust (10-fold) decrease in RAD51 protein expression (Fig. 3C) was not in agreement with results from analysis of RAD51 transcript levels using qPCR and Bru-Seq analysis, we investigated whether *PDI* KD causes ERAD-mediated degradation of RAD51. Inhibition of protein synthesis using cycloheximide (CHX) followed by evaluation of RAD51 protein levels would reveal protein decay rates in control and *PDI* KD cells. As shown in Fig. 4A and B, PDI KD resulted in a RAD51 protein half-life of approximately 2 and 6.5 hours in U87 and D54 cells, respectively, compared with 4 and 8 hours in control cells. Addition of the proteasome inhibitor MG132 rescued RAD51 protein levels in both control and *PDI* KD cells, suggesting that RAD51 is subjected to proteasome-mediated degradation (Supplementary Fig. S2). To assess whether the increased rate of RAD51 decay in the *PDI* KD cells is due to the activation of ER stress-associated degradation, we induced ER stress by treating parental GBM cells with tunicamycin and similarly observed increased protein decay rates of RAD51 (Fig. 4C and D; Supplementary Fig. S3). Taken together, our results show that induction of ER stress via either *PDI* KD or tunicamycin resulted in the reduction of RAD51 by a combination of reduced transcription

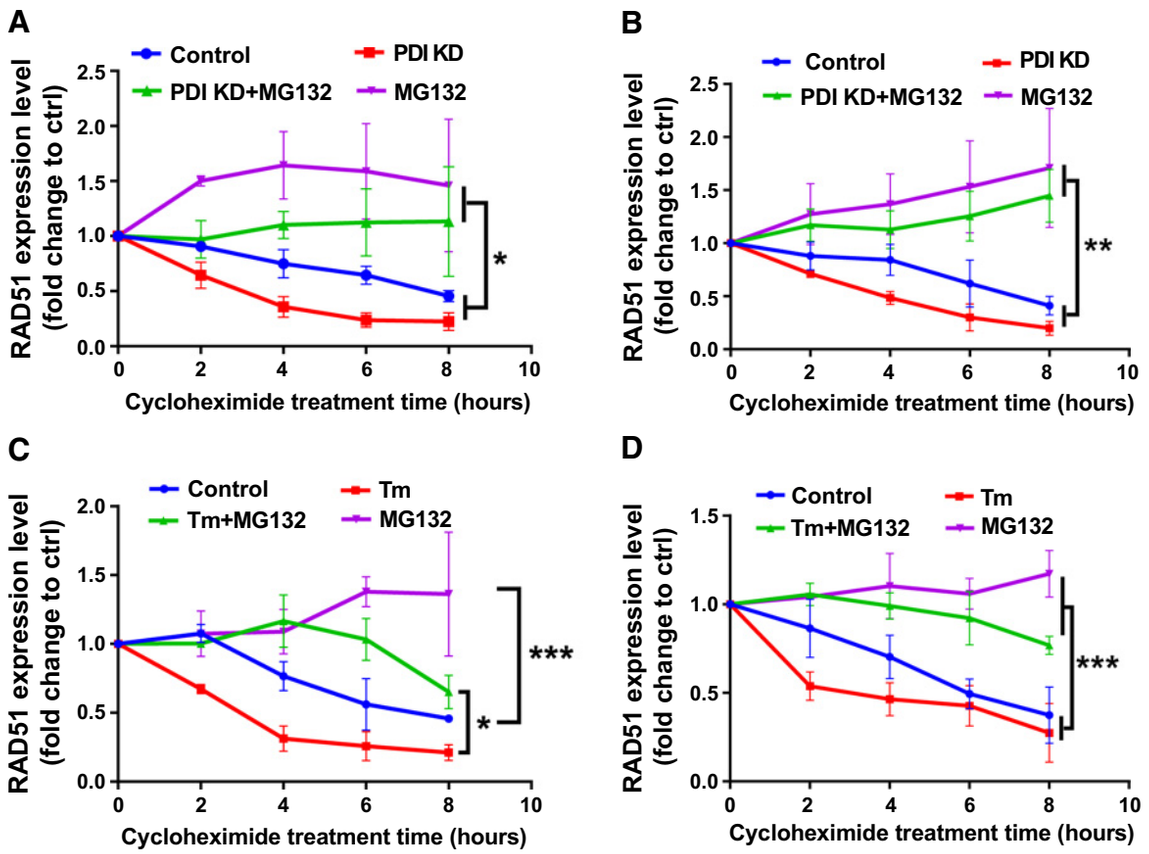

Figure 4.

ER stress leads to decreased RAD51 stability. PDI shRNA expression was induced in U87 (**A**) and D54 (**B**) cells for 48 hours in response to 2 μg/mL doxycycline. MG132 (10 μmol/L) was added for the last 16 hours of the 48-hour doxycycline treatment and the cells were prepared for Western blot analysis. Parental U87 (**C**) and D54 (**D**) cells were treated with tunicamycin (Tm; 5 μg/mL) for 16 hours prior to addition of MG132 (10 μmol/L) and cycloheximide (100 μg/mL), and cells were harvested at indicated time points for Western blot analysis. All bands were normalized against β-actin and then against corresponding control sample without cycloheximide. Data are presented as means ± SEM from three independent experiments. *, $P < 0.05$; **, $P < 0.01$; ***, $P < 0.001$.

Published OnlineFirst April 17, 2019; DOI: 10.1158/0008-5472.CAN-18-2540

and increased proteasome-mediated degradation. A decrease in RAD51 activity, as a result of transcriptional or posttranslational mechanisms, significantly compromises the ability of cells to repair DNA damage with high fidelity.

PDI KD sensitizes GBM cells to radiation

An enhanced capacity to repair damaged DNA in response to temozolomide and IR underlies the therapeutic resistance and high rate of recurrence in GBM (37). We therefore hypothesized that the observed downregulation of DNA repair enzymes (Figs. 2 and 3) in response to *PDI* KD may sensitize GBM cells to radiotherapy (IR). *PDI* KD alone inhibited cell growth by 2- and 1.3-fold in D54 and U87, respectively (Supplementary Fig. S4A). Importantly, *PDI* KD sensitized GBM cells to radiation (Fig. 5A and B) with an enhancement ratio of 1.4 ± 0.11 and 1.3 ± 0.12 in U87 and D54 cells, respectively (Supplementary Fig. S4B). Based on the central role for RAD51 in DNA double-strand break (DSB) repair (38), we explored the capacity of cells to repair IR-induced DNA damage in the presence or absence of PDI expression, using γH2AX foci formation as a surrogate for DNA DSBs. γH2AX foci were detected 30 minutes after irradiation with 2 Gy of IR in both control and *PDI* KD cells. These foci were then resolved over a 24-hour recovery period as the cells repaired the IR-induced DSBs. Importantly, the rate at which the γH2AX foci were resolved was significantly slower in the *PDI* KD cells compared with the control cells (Fig. 5C–F). Thus, the reduced transcription of DNA repair genes such as *RAD51* and ERAD-mediated protein degradation following PDI KD correlates with reduced rates of DSB repair and increased sensitivity to IR.

PDI KD sensitizes GBM xenografts to radiation

To investigate if *PDI* KD could also enhance the efficacy of radiotherapy in an *in vivo* GBM model, U87 cells expressing inducible *PDI*-targeting shRNA were implanted into the flanks of nude mice. Induction of *PDI* shRNA alone extended the tumor doubling time, from 6.8 ± 1.10 days in the control group to 11.5 $\pm$ 1.29 days in the *PDI* KD group ($P < 0.001$), whereas IR alone increased the doubling time to 16.2 ± 1.17 days (Fig. 6A and B). Despite the 3.5-fold decrease in tumor volume after doxycycline-mediated shRNA expression, the tumors eventually regrew at 12 days posttreatment termination, whereas in mice treated with IR, tumor growth was controlled until 26 days after the last treatment. Similar to our *in vitro* findings using clonogenic survival assays, *in vivo* induction of *PDI*-targeting shRNA combined with radiotherapy led to a synergistic tumor control as determined by tumor volume (4.8 ± 2.53 mm^3). In addition, this combination treatment prevented tumor regrowth for greater than 40 days post-treatment. Importantly, the combination treatment regimen was well tolerated in mice as determined by limited body weight loss (Fig. 6C). To study the mechanistic basis of *PDI* KD-mediated radiosensitization *in vivo*, two tumors from each group were harvested 1 hour after the last dose of treatment and analyzed by Western blot analysis (Fig. 6D). PDI and RAD51 expression was reduced in the doxycycline-treated tumors, and especially in

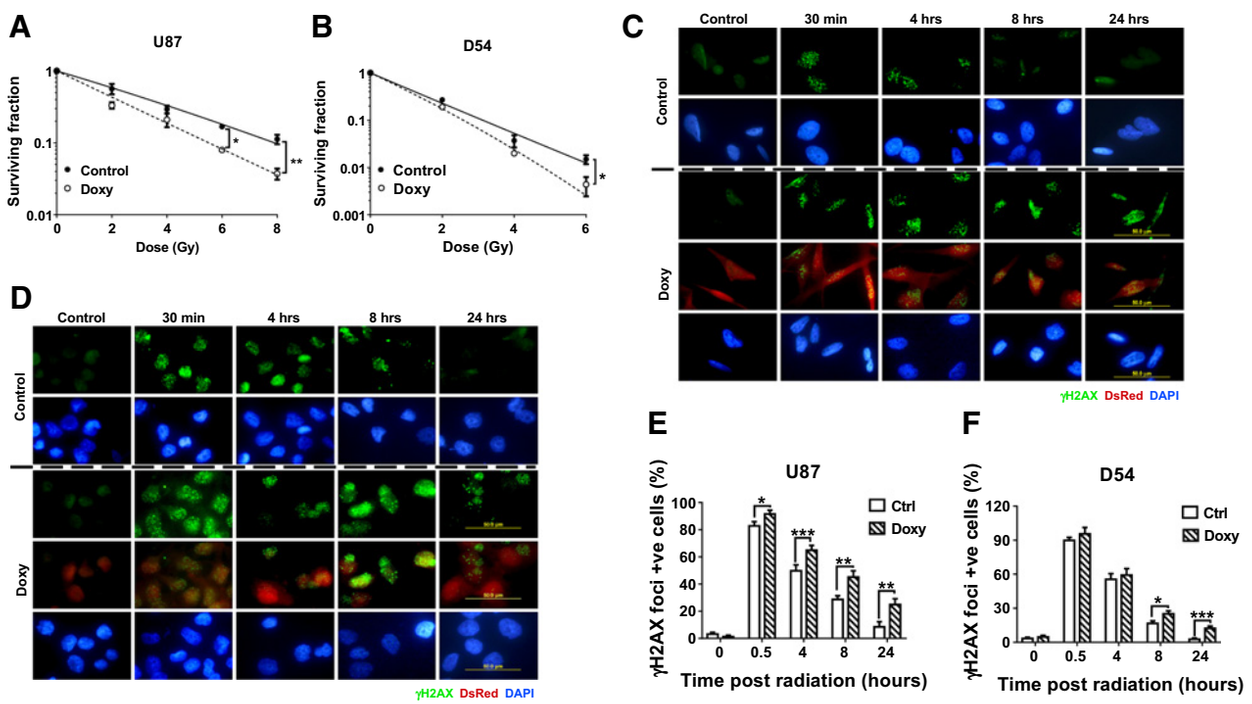

Figure 5.

KD of PDI sensitizes GBM cells to radiation. U87 (**A**) and D54 (**B**) cells were treated with 0, 2, 4, 6, or 8 Gy radiation doses and plated for clonogenic survival analysis. *PDIA1* KD was induced with 2 μg/μL doxycycline for 72 hours in U87 (**C**) and D54 (**D**). DsRed is an indicator for *PDIA1* shRNA induction. Cells were irradiated at 2 Gy, fixed, and stained with γH2AX antibody at indicated time points. Cells with ≥5γH2AX foci/nucleus were counted as positive and at least 100 cells were counted for each time point from each experiment. Quantification of γH2AX foci in U87 (**E**) and D54 (**F**). Data from three independent experiments is presented as means ± SD. *, $P < 0.05$; **, $P < 0.01$; ***, $P < 0.001$.

Published OnlineFirst April 17, 2019; DOI: 10.1158/0008-5472.CAN-18-2540

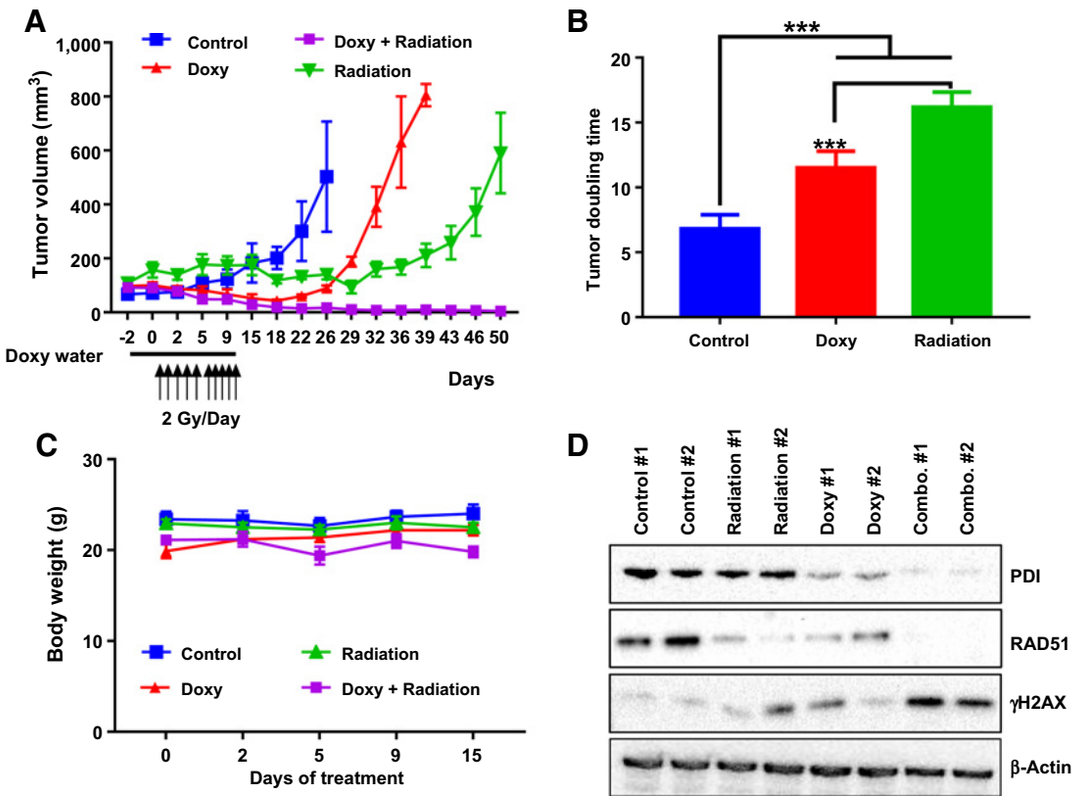

Figure 6.

KD of PDI sensitizes GBM xenografts to radiation. Approximately, a million U87 cells with inducible PDI shRNA were implanted into the flanks of nu/nu mice. When tumor volumes reached around 100 mm^3, mice were randomized into four groups and treatments: (i) control, (ii) doxycycline water (2 mg/mL in 5% sucrose water), (iii) radiation (2 Gy/day, 5 days/week), (iv) doxycycline water and radiation. The treatments were administered for 2 weeks. Doxycycline water was administered 3 days prior to radiation for combination groups. **A,** Tumors were monitored twice per week by caliper and volume was calculated as ($L \times W \times W$)/2, where W is tumor width and L is tumor length. Values were plotted as means ± SD from ≥5 mice per treatment group. **B,** Tumor doubling time was calculated according to an online calculator (http://www.chestx-ray.com/index.php/calculators/doubling-time). Tumors in the combination group never grew back, thus the doubling time for this group was infinite. **C,** Body weight recorded during treatment. **D,** Tumors from two mice from each treatment group were processed within 1 hour after the last dose of radiation and prepared for Western blot analysis.

the combination group. In addition, consistent with our *in vitro* findings, accumulation of DNA damage as evidenced by γH2AX levels was most apparent in tumors after the combination treatment, indicating a compromised ability to repair IR-induced DNA damage following *PDIA1* KD.

Discussion

Markers of ER stress are often upregulated in solid tumors and correlate with tumor stage (17). In addition, the UPR is thought to be actively involved in promoting tumor initiation and aggressive phenotypes as it participates in prosurvival processes. The prosurvival functions of the UPR are accomplished through direct regulation of protein synthesis and enhanced capacity for protein folding and posttranslational modifications within the ER (e.g., enhanced PDI activity). Furthermore, degradation of unfolded/misfolded or damaged proteins is induced by the ERAD system. Cancer cells are hypersensitive to agents that augment ER stress due to a sustained elevation of ER stress signals. ER stress–inducing compounds induce apoptosis when ER stress levels are already high (17). For example, bortezomib, a proteasome inhibitor that was approved for the treatment of multiple myeloma and mantle cell lymphoma, is an ER stress inducer. Unfortunately, studies using bortezomib as single agent or as combination therapy have not been effective in solid tumors. A promising alternative approach to induce excessive ER stress in cancer cells is to target PDI and folding of newly synthesized proteins in GBM. Indeed, we (24) and others (39, 40) have developed PDI-specific small molecule inhibitors that demonstrate significant anticancer activity. The results presented here validate PDI as a therapeutic target in GBM and demonstrate its efficacy in combination with radiotherapy through a novel mechanism involving the down-regulation of DNA repair genes important in DSB repair.

PDI KD in a mouse xenograft model of GBM increased tumor doubling time from 6.8 to 11.5 days, and radiation as a single agent resulted in a tumor doubling time of 16.2 days. The poor response to radiation in GBM is consistent with preclinical and clinical findings of the refractory nature of the disease that has been attributed to an enhance capacity of these cancer cells to repair damaged DNA (41). Our xenograft studies confirmed this with the observation that tumor recurrence occurred soon after completion of radiotherapy. Similarly, withdrawal of doxycycline

in xenografts with *PDIA1* KD caused rapid tumor repopulation, indicating that as single agents, either modality may not significantly improve the management of GBM. However, when the modalities are combined, a dramatic and prolonged effect on tumor growth rates was observed such that even at the end of the study (day 50), a majority of the animals did not have detectable tumor growth and as such, the tumor doubling time could not be determined. The enhanced efficacy of the combination therapy was also observed *in vitro* with clonogenic survival assays conducted using two independent GBM cell lines. These findings provide a rationale and guidance for lead optimization studies of current PDI inhibitors.

In an effort to delineate the mechanistic basis for the robust synergistic effect observed upon the combination of PDI inhibition with radiation, we evaluated immediate changes in gene transcription and hallmarks of ER stress. In D54 and U87 cells, expression of *PDIA1*-targeting shRNA or CRIPR/Cas9-mediated deletion of PDI expression, resulted in an increase in ER stress as detected by upregulation of BiP and phosphorylated-eIF-2α. Nascent RNA Bru-seq analysis (7) was conducted to evaluate changes in genome transcription in an unbiased manner in response to PDI inhibition and surprisingly, transcription of several DNA repair genes was downregulated following *PDI* KD (Fig. 2). Of these, RAD51 has been reported to be elevated in GBM (42), and inhibition of RAD51 using small molecules as well as siRNA sensitizes cells to DNA damaging agents (43–45). Our findings that PDI inhibition decreased expression of DNA repair genes and compromised ability to repair damaged DNA in response to IR are consistent with PDI being a promising therapeutic target for radiosensitization in GBM.

qRT-PCR studies measuring steady-state mRNA levels validated that *RAD51* transcription was slightly downregulated upon PDI inhibition. Subsequent Western blot analysis for RAD51 protein confirmed that RAD51 was strongly downregulated, and that the induction of ER stress upon tunicamycin treatment also resulted in decreased RAD51 levels. A previous study showed that RAD51 was downregulated in response to ER stress induced by tunicamycin (46). This downregulation at the protein level appeared to be caused by ubiquitin-mediated proteasomal degradation and correlated with radiosensitization of A549 lung cancer cells. In concordance with those studies, we show that ER stress caused by inhibition of PDI expression resulted in increased proteasome-mediated degradation of RAD51. Our protein stability results in the presence of cycloheximide further revealed that, despite an observed decrease in *RAD51* transcription and steady-state mRNA levels upon ER stress, the contribution of proteasomal degradation machinery was a dominant determinant of RAD51 levels, because MG132 treatment restored RAD51 to levels greater than in non-ER stressed control cells. A possible explanation is that RAD51 protein is under dynamic translational and posttranslational regulation where it is under constant proteasomal degradation as we demonstrated higher RAD51 protein level after MG132 treatment alone (Supplementary Fig. S4). In addition, the cycloheximide treatment was started after 16-hour MG132 rescue experiment, which might contribute to the higher RAD51 protein level observed compared with those without MG132 treatment.

RAD51 foci are detected in response to DNA damaging therapies that induce DSBs, including IR. Increased RAD51 protein levels are associated with therapeutic resistance and targeting of RAD51 using siRNA or Gleevec, a c-Abl inhibitor that has been shown to reduce RAD51 protein expression via inhibition of its transcription, sensitizes GBM to DNA damaging therapeutics (47, 48). RAD51 binds to single-stranded DNA at sites of the lesion to promote recombination repair in chromosomes containing a sister chromatid. Failure to repair damaged DNA in the S and G_2 phases of the cell cycle prior to mitotic entry can induce G_2 arrest or mitotic catastrophe, leading to the induction of apoptosis. Our results demonstrate that PDI KD is synergistic with radiation and specific targeting of PDI leading to ER stress and diminished levels of RAD51 provides a new therapeutic opportunity to sensitize GBM to radiotherapy.

Disclosure of Potential Conflicts of Interest

No potential conflicts of interest were disclosed.

Authors' Contributions

Conception and design: A. Pal, N. Neamati, A. Rehemtulla
Development of methodology: Y. Liu, W. Ji, A. Pal, N. Neamati
Acquisition of data (provided animals, acquired and managed patients, provided facilities, etc.): Y. Liu, J. Xu, A. Calcaterra, M. Ljungman, N. Neamati
Analysis and interpretation of data (e.g., statistical analysis, biostatistics, computational analysis): Y. Liu, A. Shergalis, J. Xu, A. Pal, M. Ljungman, N. Neamati, A. Rehemtulla
Writing, review, and/or revision of the manuscript: Y. Liu, A. Shergalis, M. Ljungman, N. Neamati, A. Rehemtulla
Administrative, technical, or material support (i.e., reporting or organizing data, constructing databases): A.M. Delaney, N. Neamati
Study supervision: N. Neamati, A. Rehemtulla

Acknowledgments

We would like to thank Drs. Dipanka Ray, Meredith Morgan, and Mr. Steven Kronenberg from Department of Radiation Oncology, University of Michigan, on their guidance on *in vitro* studies and manuscript preparation. We also want to thank University of Michigan Vector Core, Proteomics & Peptide Synthesis Core, and Microscopy & Image Analysis Laboratory for their services. A. Rehemtulla and N. Neamati received NIH CA193690 grant. This work was supported in part by the NIH Cancer Center Support Grant to the Rogel Cancer Center at the University of Michigan (P30 CA046592-29).

The costs of publication of this article were defrayed in part by the payment of page charges. This article must therefore be hereby marked *advertisement* in accordance with 18 U.S.C. Section 1734 solely to indicate this fact.

Received August 15, 2018; revised March 8, 2019; accepted April 11, 2019; published first April 17, 2019.

References

1. Thakkar JP, Dolecek TA, Horbinski C, Ostrom QT, Lightner DD, Barnholtz-Sloan JS, et al. Epidemiologic and molecular prognostic review of glioblastoma. Cancer Epidemiol Biomarkers Prev 2014;23:1985–96.
2. Stupp R, Hegi ME, Mason WP, van den Bent MJ, Taphoorn MJ, Janzer RC, et al. Effects of radiotherapy with concomitant and adjuvant temozolomide versus radiotherapy alone on survival in glioblastoma in a randomised phase III study: 5-year analysis of the EORTC-NCIC trial. Lancet Oncol 2009;10:459–66.
3. Shergalis A, Bankhead A 3rd, Luesakul U, Muangsin N, Neamati N. Current challenges and opportunities in treating glioblastoma. Pharmacol Rev 2018;70:412–45.
4. Ostrom QT, Gittleman H, Xu J, Kromer C, Wolinsky Y, Kruchko C, et al. CBTRUS statistical report: primary brain and other central nervous system

tumors diagnosed in the United States in 2009–2013. Neuro Oncol 2016; 18:v1–v75.
5. Verhaak RG, Hoadley KA, Purdom E, Wang V, Qi Y, Wilkerson MD, et al. Integrated genomic analysis identifies clinically relevant subtypes of glioblastoma characterized by abnormalities in PDGFRA, IDH1, EGFR, and NF1. Cancer Cell 2010;17:98–110.
6. Cancer Genome Atlas Research N. Comprehensive genomic characterization defines human glioblastoma genes and core pathways. Nature 2008; 455:1061–8.
7. Parsons DW, Jones S, Zhang X, Lin JC, Leary RJ, Angenendt P, et al. An integrated genomic analysis of human glioblastoma multiforme. Science 2008;321:1807–12.
8. Chinot OL, Wick W, Mason W, Henriksson R, Saran F, Nishikawa R, et al. Bevacizumab plus radiotherapy-temozolomide for newly diagnosed glioblastoma. N Engl J Med 2014;370:709–22.
9. Friedman HS, Prados MD, Wen PY, Mikkelsen T, Schiff D, Abrey LE, et al. Bevacizumab alone and in combination with irinotecan in recurrent glioblastoma. J Clin Oncol 2009;27:4733–40.
10. Rich JN, Reardon DA, Peery T, Dowell JM, Quinn JA, Penne KL, et al. Phase II trial of gefitinib in recurrent glioblastoma. J Clin Oncol 2004; 22:133–42.
11. Uhm JH, Ballman KV, Wu W, Giannini C, Krauss JC, Buckner JC, et al. Phase II evaluation of gefitinib in patients with newly diagnosed Grade 4 astrocytoma: Mayo/North Central Cancer Treatment Group Study N0074. Int J Radiat Oncol Biol Phys 2011;80:347–53.
12. Cloughesy TF, Yoshimoto K, Nghiemphu P, Brown K, Dang J, Zhu S, et al. Antitumor activity of rapamycin in a Phase I trial for patients with recurrent PTEN-deficient glioblastoma. PLoS Med 2008;5:e8.
13. Hainsworth JD, Shih KC, Shepard GC, Tillinghast GW, Brinker BT, Spigel DR. Phase II study of concurrent radiation therapy, temozolomide, and bevacizumab followed by bevacizumab/everolimus as first-line treatment for patients with glioblastoma. Clin Adv Hematol Oncol 2012;10:240–6.
14. Wilkinson B, Gilbert HF. Protein disulfide isomerase. Biochim Biophys Acta 2004;1699:35–44.
15. Cai H, Wang CC, Tsou CL. Chaperone-like activity of protein disulfide isomerase in the refolding of a protein with no disulfide bonds. J Biol Chem 1994;269:24550–2.
16. Clarke HJ, Chambers JE, Liniker E, Marciniak SJ. Endoplasmic reticulum stress in malignancy. Cancer Cell 2014;25:563–73.
17. Wang M, Kaufman RJ.The impact of the endoplasmic reticulum protein-folding environment on cancer development. Nat Rev Cancer 2014;14: 581–97.
18. Smith MH, Ploegh HL, Weissman JS. Road to ruin: targeting proteins for degradation in the endoplasmic reticulum. Science 2011;334: 1086–90.
19. Xu S, Sankar S, Neamati N. Protein disulfide isomerase: a promising target for cancer therapy. Drug Discov Today 2014;19:222–40.
20. Shin BK, Wang H, Yim AM, Le Naour F, Brichory F, Jang JH, et al. Global profiling of the cell surface proteome of cancer cells uncovers an abundance of proteins with chaperone function. J Biol Chem 2003; 278:7607–16.
21. Rho JH, Roehrl MHA, Wang JY. Glycoproteomic analysis of human lung adenocarcinomas using glycoarrays and tandem mass spectrometry: differential expression and glycosylation patterns of vimentin and fetuin a isoforms. Protein J 2009;28:148–60.
22. Zhang DH, Tai LK, Wong LL, Chiu LL, Sethi SK, Koay ESC. Proteomic study reveals that proteins involved in metabolic and detoxification pathways are highly expressed in HER-2/neu-positive breast cancer. Mol Cell Proteom 2005;4:1686–96.
23. Goplen D, Wang J, Enger PO, Tysnes BB, Terzis AJ, Laerum OD, et al. Protein disulfide isomerase expression is related to the invasive properties of malignant glioma. Cancer Res 2006;66:9895–902.
24. Xu S, Butkevich AN, Yamada R, Zhou Y, Debnath B, Duncan R, et al. Discovery of an orally active small-molecule irreversible inhibitor of protein disulfide isomerase for ovarian cancer treatment. Proc Natl Acad Sci U S A 2012;109:16348–53.
25. Xu S, Liu Y, Yang K, Wang H, Shergalis A, Kyani A, et al. Nouri Neamati Inhibition of protein disulfide isomerase in glioblastoma causes marked downregulation of DNA repair and DNA damage response genes. Theranostics 2019;9:2282–98.
26. Galligan JJ, Petersen DR. The human protein disulfide isomerase gene family. Hum Genomics 2012;6:6.
27. Bao S, Wu Q, McLendon RE, Hao Y, Shi Q, Hjelmeland AB, et al. Glioma stem cells promote radioresistance by preferential activation of the DNA damage response. Nature 2006;444:756–60.
28. Bigner SH, Bullard DE, Pegram CN, Wikstrand CJ, Bigner DD. Relationship of in vitro morphologic and growth characteristics of established human glioma-derived cell lines to their tumorigenicity in athymic nude mice. J Neuropathol Exp Neurol 1981;40:390–409.
29. Sanjana NE, Shalem O, Zhang F. Improved vectors and genome-wide libraries for CRISPR screening. Nat Methods 2014;11:783–84.
30. Shalem O, Sanjana NE, Hartenian E, Shi X, Scott DA, Mikkelson T, et al. Genome-scale CRISPR-Cas9 knockout screening in human cells. Science 2014;343:84–87.
31. Paulsen MT, Veloso A, Prasad J, Bedi K, Ljungman EA, Magnuson B, et al. Use of Bru-Seq and BruChase-Seq for genome-wide assessment of the synthesis and stability of RNA. Methods 2014;67:45–54.
32. Liu Y, Burness ML, Martin-Trevino R, Guy J, Bai S, Harouaka R, et al. RAD51 mediates resistance of cancer stem cells to PARP inhibition in triple-negative breast cancer. Clin Cancer Res 2017;23:514–22.
33. Lee AS. The ER chaperone and signaling regulator GRP78/BiP as a monitor of endoplasmic reticulum stress. Methods 2005;35:373–81.
34. Teske BF, Wek SA, Bunpo P, Cundiff JK, McClintick JN, Anthony TG, et al. The eIF2 kinase PERK and the integrated stress response facilitate activation of ATF6 during endoplasmic reticulum stress. Mol Biol Cell 2011;22: 4390–405.
35. Han J, Kaufman RJ. Physiological/pathological ramifications of transcription factors in the unfolded protein response. Genes Dev 2017;31: 1417–38.
36. Adamson B, Smogorzewska A, Sigoillot FD, King RW, Elledge SJ. A genome-wide homologous recombination screen identifies the RNA-binding protein RBMX as a component of the DNA-damage response. Nat Cell Biol 2012;14:318–28.
37. Erasimus H, Gobin M, Niclou S, Van Dyck E. DNA repair mechanisms and their clinical impact in glioblastoma. Mutat Res Rev Mutat Res 2016;769: 19–35.
38. Baumann P, Benson FE, West SC. Human Rad51 protein promotes ATP-dependent homologous pairing and strand transfer reactions in vitro. Cell 1996;87:757–66.
39. Vatolin S, Phillips JG, Jha BK, Govindgari S, Hu J, Grabowski D, et al. Novel protein disulfide isomerase inhibitor with anticancer activity in multiple myeloma. Cancer Res 2016;76:3340–50.
40. Kaplan A, Gaschler MM, Dunn DE, Colligan R, Brown LM, Palmer AG 3rd, et al. Small molecule-induced oxidation of protein disulfide isomerase is neuroprotective. Proc Natl Acad Sci U S A 2015;112:E2245–52.
41. Atkins RJ, Ng W, Stylli SS, Hovens CM, Kaye AH. Repair mechanisms help glioblastoma resist treatment. J Clin Neurosci 2015;22:14–20.
42. Welsh JW, Ellsworth RK, Kumar R, Fjerstad K, Martinez J, Nagel RB, et al. Rad51 protein expression and survival in patients with glioblastoma multiforme. Int J Radiat Oncol Biol Phys 2009;74:1251–5.
43. Lim YC, Roberts TL, Day BW, Stringer BW, Kozlov S, Fazry S, et al. Increased sensitivity to ionizing radiation by targeting the homologous recombination pathway in glioma initiating cells. Mol Oncol 2014;8:1603–15.
44. Short SC, Giampieri S, Worku M, Alcaide-German M, Sioftanos G, Bourne S, et al. Rad51 inhibition is an effective means of targeting DNA repair in glioma models and CD133+ tumor-derived cells. Neuro Oncol 2011;13: 487–99.
45. King HO, Brend T, Payne HL, Wright A, Ward TA, Patel K, et al. RAD51 Is a Selective DNA repair target to radiosensitize glioma stem cells. Stem Cell Rep 2017;8:125–39.
46. Yamamori T, Meike S, Nagane M, Yasui H, Inanami O. ER stress suppresses DNA double-strand break repair and sensitizes tumor cells to ionizing radiation by stimulating proteasomal degradation of Rad51. FEBS Lett 2013;587:3348–53.
47. Russell JS, Brady K, Burgan WE, Cerra MA, Oswald KA, Camphausen K, et al. Gleevec-mediated inhibition of Rad51 expression and enhancement of tumor cell radiosensitivity. Cancer Res 2003;63:7377–83.
48. Golding SE, Rosenberg E, Khalil A, McEwen A, Holmes M, Neill S, et al. Double strand break repair by homologous recombination is regulated by cell cycle-independent signaling via ATM in human glioma cells. J Biol Chem 2004;279:15402–10.

Published OnlineFirst April 17, 2019; DOI: 10.1158/0008-5472.CAN-18-2540

Cancer Research
The Journal of Cancer Research (1916–1930) | The American Journal of Cancer (1931–1940)

AACR American Association for Cancer Research

Activation of the Unfolded Protein Response via Inhibition of Protein Disulfide Isomerase Decreases the Capacity for DNA Repair to Sensitize Glioblastoma to Radiotherapy

Yajing Liu, Wenbin Ji, Andrea Shergalis, et al.

Cancer Res 2019;79:2923-2932. Published OnlineFirst April 17, 2019.